

# Supplementary Information

## Color Imaging *via* Nearest Neighbor Hole Coupling in Plasmonic Color Filters Integrated onto a Complementary Metal-Oxide Semiconductor Image Sensor

Stanley P. Burgos,<sup>†,§</sup> Sozo Yokogawa,<sup>†,‡,§</sup> and Harry A. Atwater<sup>†,\*</sup>

<sup>†</sup>California Institute of Technology, 1200 East California Boulevard, Pasadena, California 91125, United States, and

<sup>‡</sup>Sony Corporation, Atsugi Tec. 4-14-1 Asahi-cho, Atsugi, Kanagawa 243-0014, Japan.

<sup>§</sup>Equal author contribution.

\*Address correspondence to haa@caltech.edu.

### SUPPLEMENTARY FIGURES

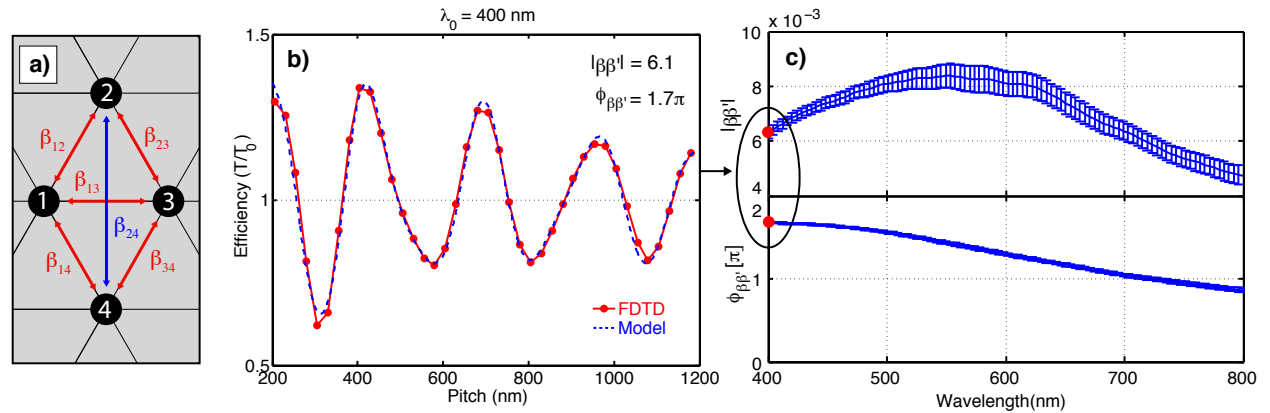


**Figure S1. (b) Transmission efficiency as a function of pitch for a symmetric 4-hole triangular-lattice unit cell (a), consisting of 180 nm diameter holes set at a pitch of 340 nm in a 150 nm thick Al film embedded in SiO<sub>2</sub>. The red dotted spectrum is extracted from FDTD simulations and the blue dashed spectrum corresponds to the fitted scattering-absorption model. The horizontal dashed curve at ‘1’ corresponds to the normalized transmission efficiency of a single isolated hole. (c) Spectrally resolved scattering-absorption parameters obtained by varying the wavelength from 400–800 nm and fitting as done in (b).**

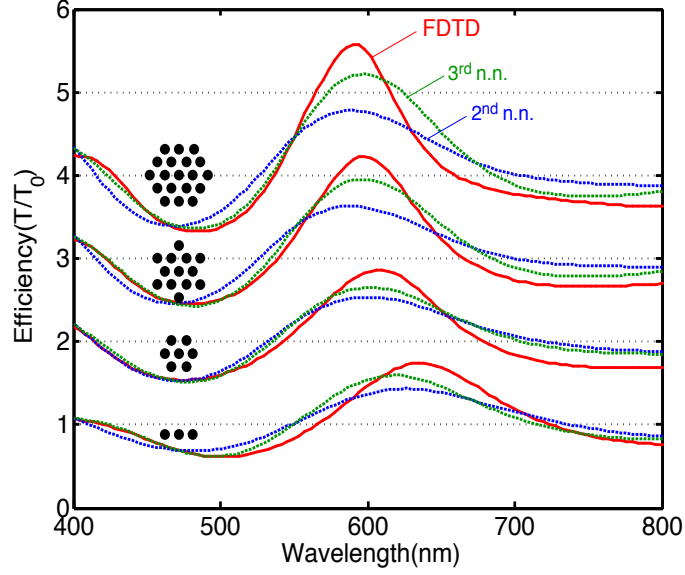


**Figure S2.** Transmission efficiency for different hole array configurations as a function of number of contributing nearest neighbors (n.n.). Data is shown for spectra calculated with FDTD as well as with the nearest-neighbor scattering model with second and third n.n. contributions. The hole array configurations (see insets) consist of 180 nm diameter holes set at a pitch of 380 nm in a 150 nm thick Al film embedded in SiO<sub>2</sub>.

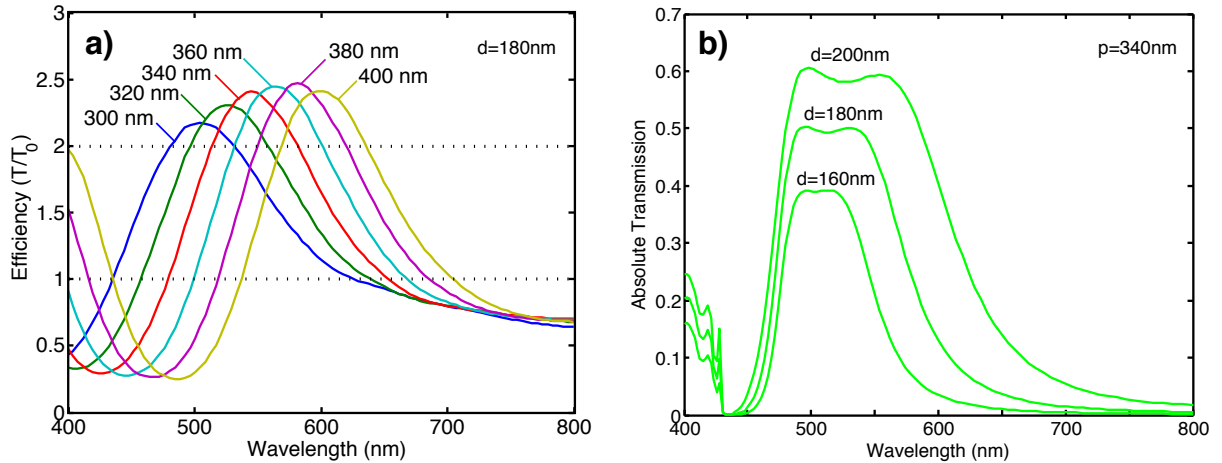


**Figure S3.** (a) Normalized transmission efficiency curves extracted from the scattering model as a function of array pitch for a  $\sim 10 \times 10 \mu\text{m}^2$  square-shaped triangular-lattice hole array consisting of 180 nm diameter holes in a 150 nm thick Al film embedded in SiO<sub>2</sub>. (b) Absolute transmission efficiency extracted from FDTD for an infinite triangular-lattice hole array as a function of hole diameter for an array consisting of 340 nm pitch holes in a 150 nm Al film embedded in SiO<sub>2</sub>.

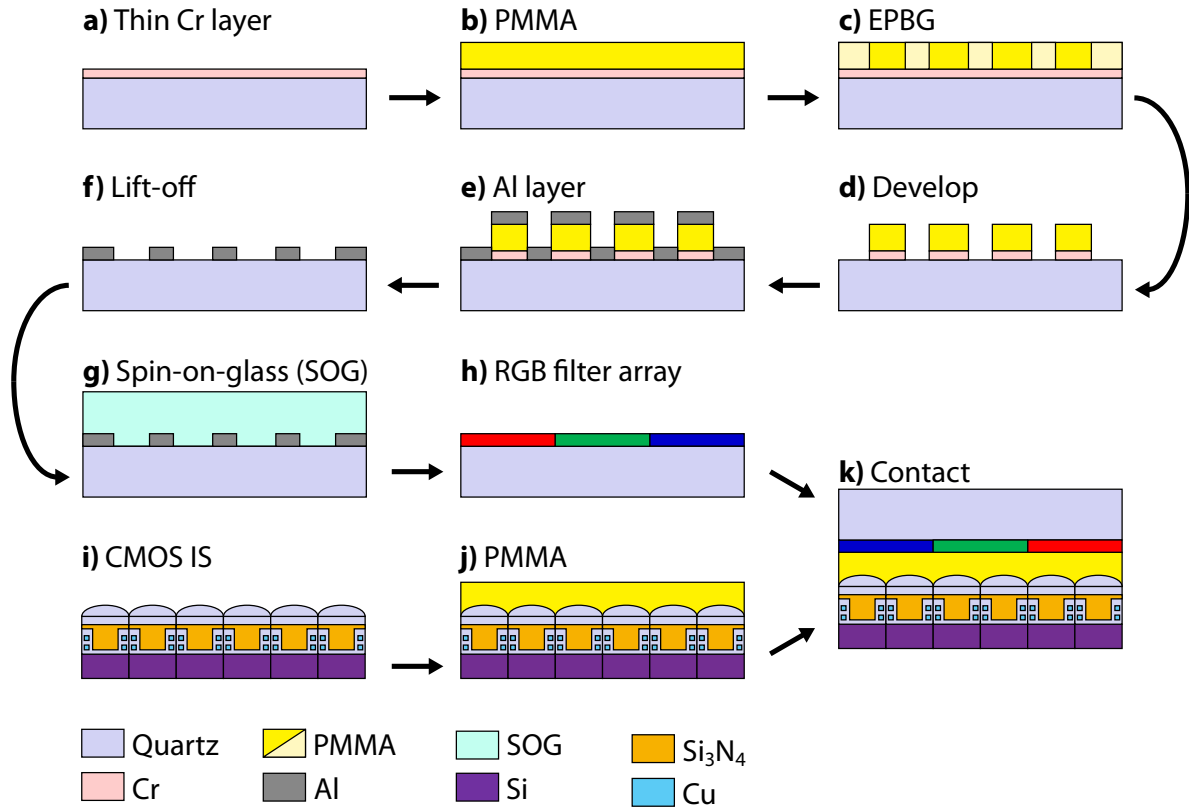


**Figure S4. Fabrication and integration of hole array filter with CMOS image sensor.** (a) Thin layer of Cr is deposited on quartz substrate to reduce charging during electron-beam writing of the hole array color filter pattern. (b) PMMA is spin coated on top of Cr layer. (c) PMMA is exposed using electron-beam lithography. (d) Exposed PMMA pattern is developed. (e) Al layer is deposited to form hole array pattern. (f) PMMA is lifted off. (g) Spin-on-glass (SOG) is spin coated over Al pattern. (h) Resulting pattern is RGB hole array color filter in Bayer layout. (i) CMOS image sensor is (j) spin coated with PMMA to planarize the microlenses. (k) Hole array filter is contacted onto planarized CMOS IS.

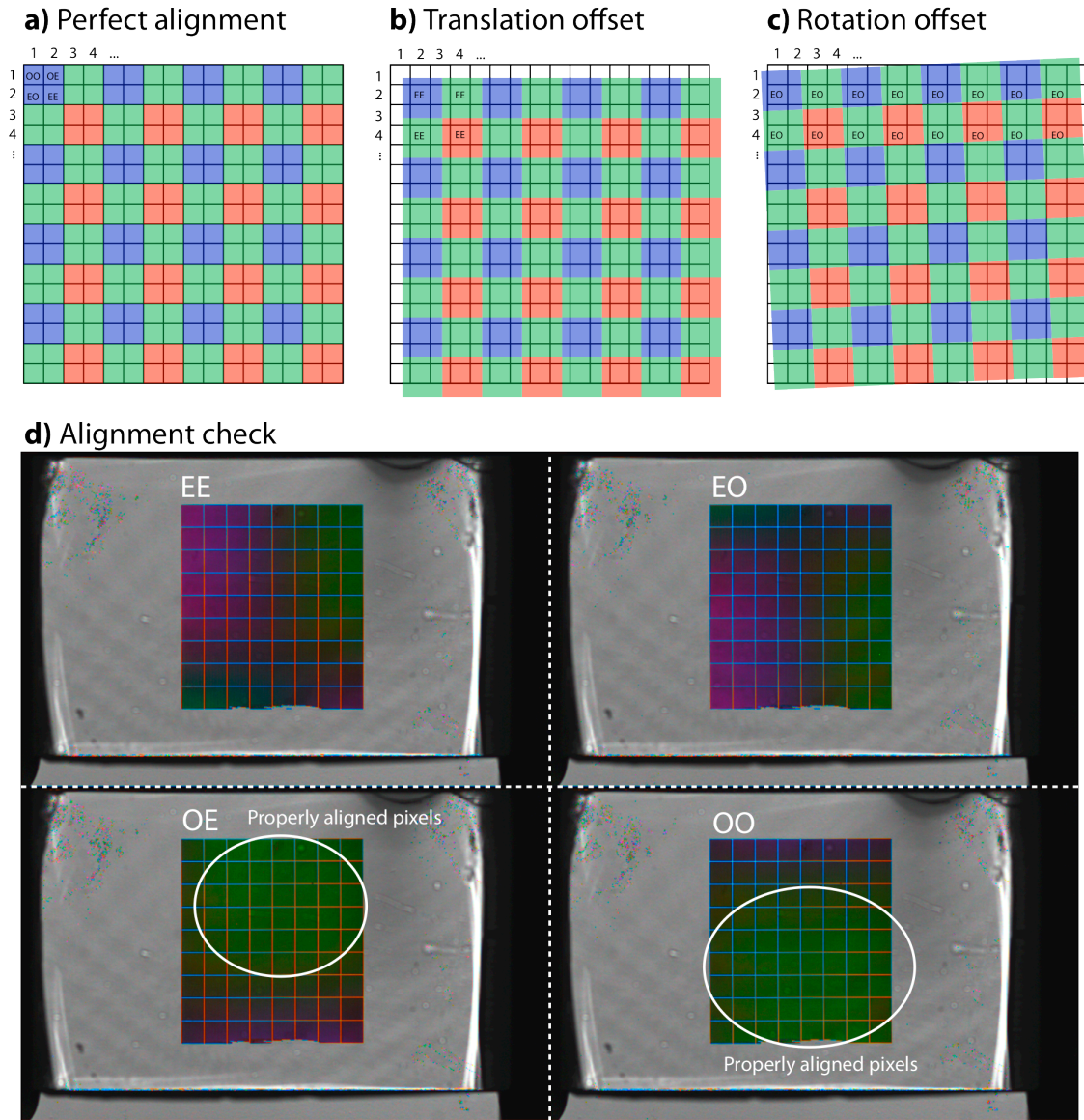


**Figure S5. Alignment of plasmonic hole array filter with CMOS image sensor.** The lined grid represents the pixel array of the CMOS image sensor and the transparent RGB box grid represents the plasmonic hole array color filter array in Bayer layout. The pixels are labeled using matrix convention  $(i, j)$  with  $i$  coming from the horizontal axis and  $j$  coming from the vertical axis, and the double letters inside of the grid refer to the parity of the pixel label, with E for even and O for odd. Pixel and filter array are shown with (a) perfect alignment, (b) translational offset, and (c) rotational offset. (d) Image readout of the difference parity set of pixels: even-even (EE), even-odd (EO), odd-even (OE), and odd-odd (OO), after demosaicing a gray wall image taken with the CMOS image sensor integrated with the aligned hole array color filters.



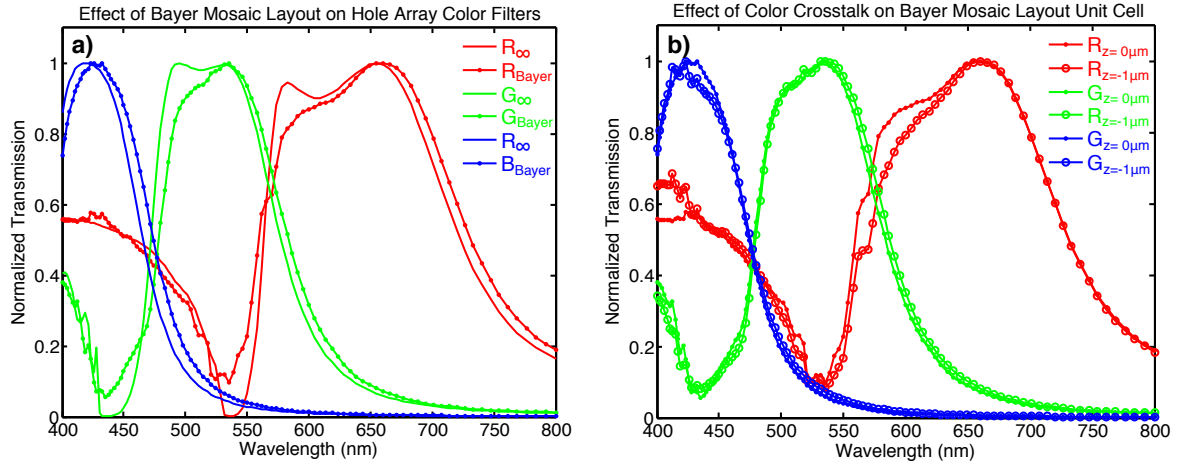


**Figure S6. Normalized FDTD-calculated transmission efficiencies for triangular-lattice hole arrays corresponding to red ( $p = 420$  nm,  $d = 240$  nm), green ( $p = 340$  nm,  $d = 180$  nm), and blue ( $p = 260$  nm,  $d = 140$  nm) filters in a 150 nm Al film embedded in  $\text{SiO}_2$ . (a) Transmission response of a periodic  $11.2 \times 11.2 \mu\text{m}^2$  RGB hole array color filter Bayer unit cell (similar to that shown in Fig. S2b, comprised of  $5.6 \times 5.6 \mu\text{m}^2$  RGB hole array color filters with zero separation between color patches) compared to the transmission of infinite RGB hole array filters (simulated with Bloch boundary conditions as described in Methods). (b) Transmission response of a periodic  $11.2 \times 11.2 \mu\text{m}^2$  RGB hole array color filter Bayer unit cell in which the transmission for each color filter is monitored both right underneath the Bayer unit cell ( $z = 0 \mu\text{m}$ ) and at  $z = -1 \mu\text{m}$ , where the focusing micro-lenses are located in the device simulations. The transmission of each color filter is monitored with a set of transmission monitors that have physical extent corresponding to the physical size of the corresponding RGB color filters, thus corresponding to the amount of light captured by the micro-lenses of each color filter.**

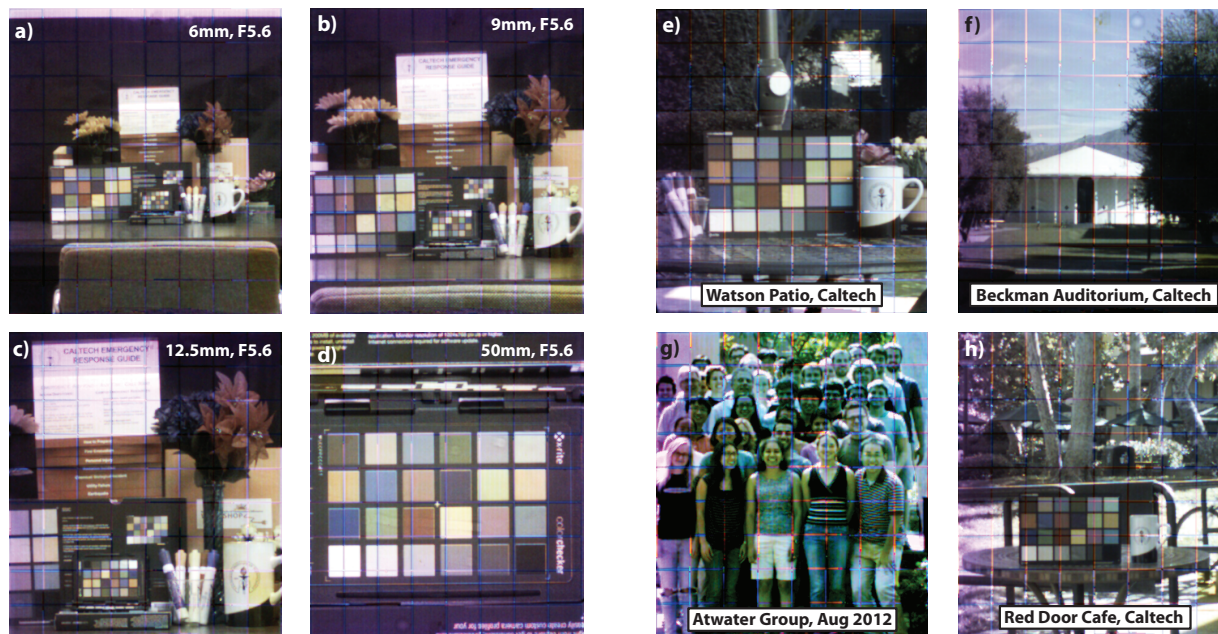


**Figure S7. Focal length dependence and outdoor lighting conditions.** Images of 24-color Macbeth chart positioned in a scene taken with CMOS image sensor integrated with RGB plasmonic hole array filter with a 5.6 f-number and a (a) 6 mm, (b) 9 mm, (c) 12.5 mm, and (d) 50 mm lens. Images taken with outdoor lighting conditions of (e) Watson Patio, Caltech, (f) Beckman Auditorium, Caltech, (g) Atwater Group, Aug. 2012, Caltech, and (h) Red Door Café, Caltech.